Desalination and Water Treatment
www.deswater.com

doi: 10.1080/19443994.2016.1168579

57 (2016) 26507–26517
November

Taylor & Francis
Taylor & Francis Group

Mechanical vapor compression—Membrane distillation hybrids for reduced specific energy consumption

Jaichander Swaminathan, Kishor G. Nayar, John H. Lienhard V*

Rohsenow Kendall Heat Transfer Laboratory, Department of Mechanical Engineering, Massachusetts Institute of Technology, 77 Massachusetts Avenue, Cambridge, MA 02139-4307, USA, email: lienhard@mit.edu (J.H. Lienhard V)

Received 1 January 2016; Accepted 13 March 2016

ABSTRACT

The energy efficiency of membrane distillation (MD) systems is low when compared to other thermal desalination systems. This leads to high water production costs when conventional fuels such as natural gas are used. In MD, separation of pure product water from feedwater is driven by differences in vapor pressure between the streams. Thus, the process can occur at low temperature and ambient pressure. As a result, MD is most frequently paired with waste or renewable sources of low temperature heat energy that can be economically more feasible. MD systems with internal heat regeneration have been compared to and modeled similar to counter-flow heat exchangers. In this study, MD is used to replace the preheater heat exchanger used for thermal energy recovery from the brine stream in mechanical vapor compression (MVC). Using MD in place of the heat exchanger results not only in effectively free thermal energy for MD, but also subsidized cost of capital, since the MD module is replacing expensive heat exchanger equipment. The MVC–MD hybrid system can lead to about 6% decrease in cost of water, compared to a stand-alone MVC system. The savings increase with: an increase in MVC operating temperature, a decrease in MVC recovery ratio, and with a decrease in MD capital cost. The conductive gap configuration of MD leads to maximum savings, followed by air gap and permeate gap systems, over a range of operating conditions, assuming equal specific cost of capital for these configurations.

Keywords: Membrane distillation; Mechanical vapor compression; Energy recovery; Heat exchanger

1. Introduction

1.1. Membrane distillation

Membrane distillation (MD) is a thermal desalination technology, in which separation of pure water happens through evaporation of pure water from a warm contaminated or salty solution. Direct contact and vacuum MD systems incorporate feed preheating and energy recovery in external heat exchangers [1,2]. Multistage configurations of vacuum MD have also been implemented to improve its energy efficiency and water recovery [3]. In single-stage membrane distillation systems with internal heat recovery,

*Corresponding author.

Presented at the IDA 2015 World Congress (Desaltech 2015) 29 August–4 September, 2015 San Diego, CA, USA

such as air gap (AGMD), permeate gap (PGMD), and conductive gap membrane distillation (CGMD), the vapor condenses in the gap between the membrane and a condensing surface. The energy released upon condensation is transferred through the condensing surface into a cooler stream. The cooler stream is often the feed itself, being preheated to achieve energy recovery. Fig. 1 shows a schematic diagram of the MD process as well as the typical temperature profiles of the hot and cold streams within the system along the length direction. The two streams are in a counter-flow configuration. Overall, the temperature profile is similar to what is seen in a counter-flow heat exchanger.

MD is a relatively expensive desalination technology due to its low energy efficiency [4–6], leading to a large cost of in terms thermal energy. In addition, the membrane capital and replacement costs may also be significant due to fouling and inorganic salt precipitation with some feed solutions [7]. Pumping power for circulating the feed and coolant streams through the module is usually a smaller part of the total cost. As a result, MD has usually been targeted at applications with availability of a waste thermal energy source [8].

In AGMD, air fills the gap between the membrane and condensing surface, with the pure product forming a film on the condensing surface. In PGMD, the gap is filled with pure water and in the case of CGMD [9,10], the thermal conductance of the gap is enhanced in such a way that the gap no longer constitutes the major thermal resistance within the MD module. In this study, the gap depth for all three systems is assumed to be 1 mm. The thermal conductivity of the gap is assumed to be equal to that of pure water at 0.6 W/m-K for PGMD and 10 W/m-K for CGMD. (An alternative method of realizing CGMD would be to reduce the gap depth to about 0.06 mm without enhanced conductivity).

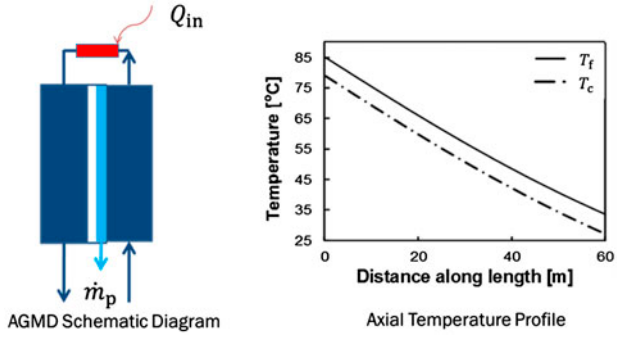

Fig. 1. MD schematic diagram and internal temperature profiles.

1.2. Mechanical vapor compression

Mechanical vapor compression (MVC) desalination is a work-driven desalination process. MVC has been modeled in detail and analyzed by various researchers [6,11–14]. Mistry et al. [6] analyzed the entropy generation in various seawater desalination technologies and found that after reverse osmosis (RO), MVC had the highest second law efficiency.

An MVC system primarily consists of preheater heat exchangers, a mechanical vapor compressor, and an evaporator/condenser unit. Fig. 2 shows a schematic diagram of a single-effect MVC process where work input to the mechanical compressor causes vapor from the evaporator/condenser unit to be compressed. The compression increases the saturation temperature of the vapor stream and also raises the vapor temperature to a superheated state. The evaporator/condenser unit typically consists of a falling film shell-and-tube heat exchanger where feed seawater is sprayed over the outside of the tubes. Hot compressed vapor from the compressor flows within the tubes while the cooler feed seawater flows outside the tubes. Heat transfer from the vapor to the feed seawater causes vapor to condense inside the tube and form pure water, and also causes some of the feed seawater to evaporate. The vapor is then removed and compressed by the compressor and passed back inside the tubes. Both the pure product water and brine streams exiting the evaporator/condenser unit leave at temperatures much higher than the ambient temperature. The thermal energy in these streams is recovered within the MVC process using heat exchangers to preheat the incoming feed stream. The incoming feed stream is split into two parts corresponding to the flow rates of the pure water and brine and passed through the heat exchangers. The preheated streams are then mixed together before being introduced into evaporator vessel.

1.3. Proposed concept: MVC–MD hybrid

In this paper, we propose the concept of hybridizing MVC with MD for desalination of seawater. Instead of using a conventional heat exchanger for recovering thermal energy from the brine stream and preheating the feed seawater stream, we propose using MD. Fig. 3 shows a schematic diagram of the proposed MVC–MD hybrid system. Only the brine-feed heat exchanger is replaced with the MD module. Since the distillate stream is already pure water, a simple heat exchanger is sufficient to recover energy from this stream. The main motivation for hybridizing MD and MVC is to achieve additional desalination and pure water production, when heat energy is transferred from the brine to the

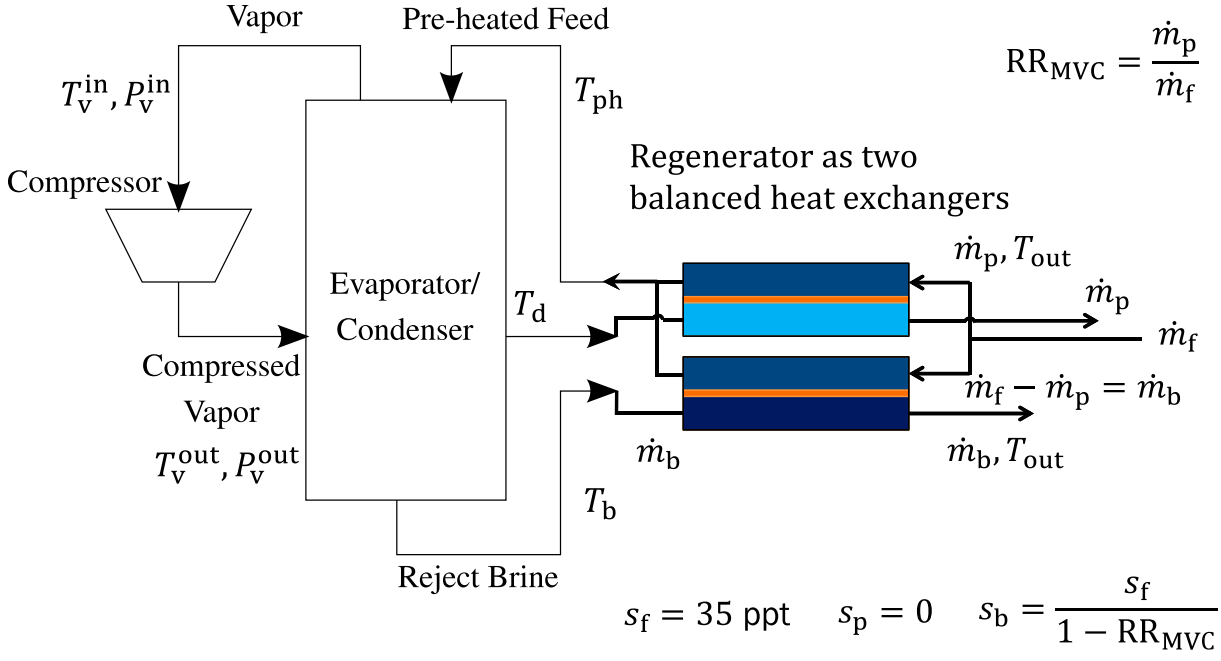

Fig. 2. MVC system for desalination of seawater.

incoming feed. The thermal energy for the MD section of the hybrid system is truly "free." This is in contrast to other "waste-heat" sources for MD, where additional capital cost is associated with introducing heat exchangers to harness this waste heat. In addition to the fact that the thermal energy is free, the cost of capital for the MD system is also offset by the cost of the heat exchanger that the MD module is replacing. If the marginal cost of the additional water produced in the MD section is lower than the specific cost of water from MVC, an overall net cost benefit results from using an MVC–MD hybrid system.

2. Methodology

2.1. Numerical modeling

The numerical modeling is carried out using a simultaneous equation solver, Engineering Equation Solver [15].

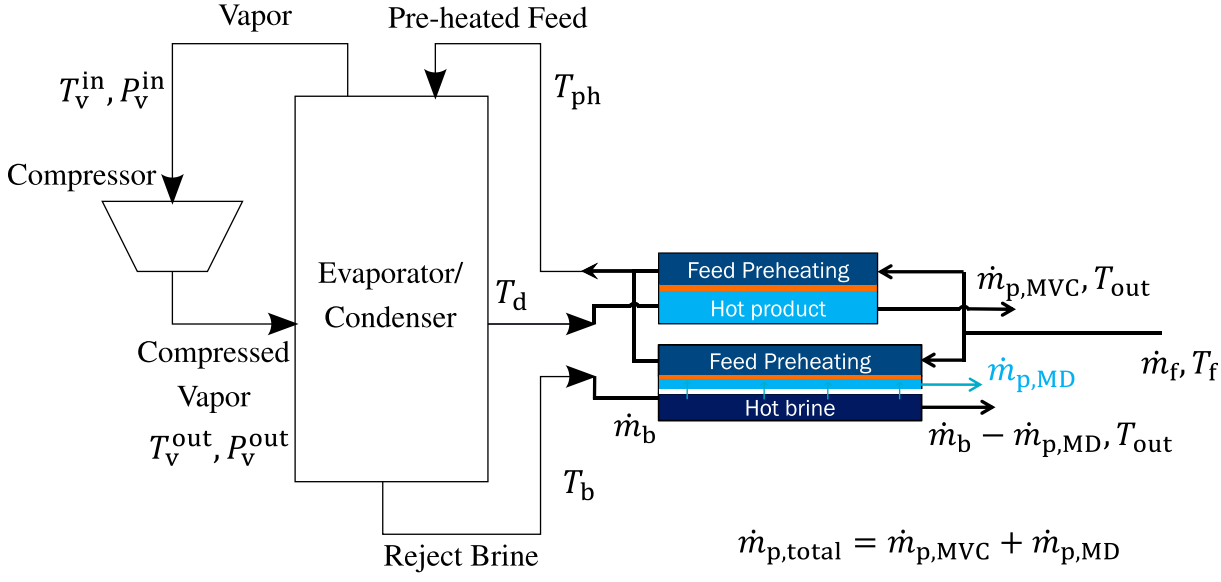

Fig. 3. MVC–MD hybrid system with MD replacing the reject brine regenerator.

2.1.1. Membrane distillation

The modeling methodology for MD is presented in detail elsewhere [4,9]. The key features of the model along with some modifications are discussed briefly here. The flux, J, through the membrane is proportional to the vapor pressure difference across the membrane:

$$J = B \times \Delta p_{\text{vap}}^{\text{m}} \tag{1}$$

The membrane permeability or transfer coefficient (B) is set at 10^{-6} kg/m^2-s-Pa [4,5].

The vapor pressure on the feed side is a function of the feed temperature at the membrane as well as the salinity of the solution at the feed–membrane interface:

$$p_{\text{vap}}^{\text{f,m}} = P_{\text{sat}}\left(T_{\text{f,m}}\right) \times a_{\text{w}}\left(T_{\text{f,m}}, s_{\text{f,m}}\right) \tag{2}$$

where a_{w} is the activity of water as a function of temperature and salinity.

The temperature at the feed membrane interface is lower than the temperature of the feed bulk and the salinity at the feed membrane interface is higher than the salinity of the bulk feed due to the temperature and concentration boundary layer resistances. These differences are captured through the heat and mass transfer coefficients within the channels and using the film model of concentration polarization [16].

The brine solution is approximated as sodium chloride solution. The effect of salinity on specific heat capacity is considered through a curve-fit based on properties of sodium chloride solution at 60°C using the Pitzer model described in Thiel et al. [17]:

$$c_{\text{P}} = 15.556 \times m^2 - 241.78 \times m + 4161.9 \tag{3}$$

where c_{P} is the specific heat capacity of the solution in J/kg-K and m is the molality of NaCl.

One important parameter to note is the thermal efficiency of the MD process (η). η is a measure of the fraction of total energy transferred between the hot and cold streams through mass transfer. For a simple heat exchanger, η is equal to 0. A higher value of η indicates more pure water production in the MD section, for the same amount of total heat transferred from the hot side to the cold side. At any local section of the MD module:

$$\eta = \frac{Jh_{\text{fg}}}{Jh_{\text{fg}} + \dot{q}_{\text{cond}}} \tag{4}$$

where h_{fg} is the enthalpy of evaporation and $\dot{q}_{\text{cond}}$ is the heat flux by conduction through the membrane and is given by $\left(\frac{k_{\text{m}}}{\delta_{\text{m}}} \times \Delta T_{\text{m}}\right)$.

Swaminathan et al. [10] showed that AGMD has higher η than PGMD and CGMD under similar operating conditions, as a result of the air gap. On the other hand, to achieve the same amount of total heat transfer, AGMD would need a larger membrane area due to the lower overall heat transfer coefficient, followed by PGMD and then CGMD. Swaminathan et al. also showed that for representative designs at the same value of GOR, AGMD uses approximately two times the amount of membrane area, leading about 50% lower flux compared to CGMD. Using AGMD in the place of the brine-feed heat exchanger would therefore lead to a higher pure water production rate than CGMD, while requiring larger area than CGMD. The overall effect of these two factors on the cost savings is discussed in Section 3.5.

2.1.2. Mechanical vapor compression

An analytical model originally developed by El-Dessouky and Ettouney [11] was used for simulating MVC. Key design inputs were also taken from other references [6,14,18]. The inputs to the model are given in Table 1.

The key assumptions in the model are:

(1) Brine and product water exit the preheaters into the environment at the same temperature, T_{out}.
(2) Rejected brine is assumed to leave at the boiling point of the feed in the evaporator.
(3) Specific heat capacity of seawater is approximated by that of aqueous sodium chloride, described by Eq. (3).
(4) Boiling point elevation (BPE) is calculated using a correlation for sodium chloride solutions as a function of salinity and temperature [17].
(5) The mass flow rate of the feed is split between each heat exchanger in the preheater such that each heat exchanger is balanced (i.e. the driving temperature difference is constant along

Table 1
Summary of inputs to MVC model

Feed salinity	35 ppt
MVC recovery ratio (RR_{MVC})	0.4–0.87
Product salinity	0 ppt
Feed inlet temperature (T_{f})	25°C
Top brine temperature (T_{MVC})	50–90°C
Evaporator terminal temperature difference (TTD)	3 K
Isentropic compressor efficiency (η_{comp})	0.7

the length of the heat exchanger). The split feed streams recombine after the preheater such that the average temperature is T_{ph}.

(6) Complete condensation is assumed in the condenser so that fluid leaving the condenser is a saturated liquid at temperature T_d.

(7) Vapor entering the compressor is assumed to be saturated.

The recovery ratio of the MVC system relates the mass flow rates of the feed ($\dot{m}_f$) to that of the product water ($\dot{m}_p$) as:

$$RR_{MVC} = \frac{\dot{m}_p}{\dot{m}_f} \tag{5}$$

The "top brine temperature" (T_{MVC}), as the name suggests, is the highest temperature attained by the brine in the system. This is equivalent to the boiling point of the feed in the evaporator (T_{evap}) and the temperature of the brine leaving the evaporator (T_b), and it is an input to the model. The temperature at which vapor from the compressor condenses is given by:

$$T_{cond} = T_{evap} + TTD \tag{6}$$

where TTD is the terminal temperature difference in the evaporator; TTD is also an input to the model. The corresponding pressures in the evaporator and condenser are given by:

$$P_{evap} = P_{sat,w}(T_{evap} - BPE) \tag{7}$$

$$P_{cond} = P_{sat,w}(T_{cond}) \tag{8}$$

where $P_{sat,w}$ is the saturation vapor pressure of pure water.

The energy balance in the evaporator/condenser unit is given by:

$$\dot{Q}_{evap} = \dot{m}_f\, c_{P,f}\left(T_{evap} - T_{ph}\right) + \dot{m}_d\, h_{fg,evap} \tag{9}$$

$$\dot{Q}_{cond} = \dot{m}_d(h_{fg,cond} + c_{P,v}\Delta T_{suph}) \tag{10}$$

$$\dot{Q}_{evap} = \dot{Q}_{cond} \tag{11}$$

where $\dot{Q}_{evap}$ is the rate of heat transfer in the evaporator, $\dot{m}_f$ is the mass flow rate of the feed, $c_{p,f}$ is the specific heat capacity of the saline feed, T_{ph} is the temperature of the preheated feed coming in to the evaporator, $\dot{m}_d$ is the mass flow rate of the distillate produced in the condenser (from mass conservation, equivalent to the vapor produced in the evaporator and compressed by the compressor), $h_{fg,evap}$ is the latent heat of vaporization in the evaporator, $\dot{Q}_{cond}$ is the rate of heat transfer in the condenser, $h_{fg,cond}$ is the latent heat of vaporization in the condenser, $c_{p,v}$ is the specific heat capacity of water vapor, and ΔT_{sup} is the amount to which vapor in the compressor gets superheated. The latter is given by:

$$\Delta T_{sup} = T_v^{out} - T_{cond} \tag{12}$$

Solving Eqs. (6)–(8) gives the temperature of the preheated feed (T_{ph}) before it enters the evaporator. T_v^{out} is calculated from the known values for the compressor's isentropic efficiency and the pressures in the evaporator and condenser.

The energy balance on the preheaters is given by:

$$\begin{aligned}\dot{Q}_{ph} &= \dot{m}_f\, c_{P,f}\left(T_{ph} - T_f\right) \\ &= \dot{m}_b c_{P,b}(T_b - T_{out}) + \dot{m}_p c_{P,w}(T_d - T_{out})\end{aligned} \tag{13}$$

where $\dot{Q}_{ph}$ is the total heat transfer rate in the preheater; $c_{P,f}$, $c_{P,b}$ and $c_{P,w}$ are the specific heat capacities of the saline feed, brine and that of pure water, respectively; $\dot{m}_f$, $\dot{m}_b$ and $\dot{m}_p$ are the mass flow rates of the feed, brine, and product water (i.e. distillate); T_b, and T_d are the temperature at which the brine and the product water, respectively, leave the evaporator/condenser unit, while T_{out} is the temperature at which the brine and the product water exits the preheater into the environment. Solving the above energy balance gives the value of T_{out}.

The log mean temperature difference in each of the balanced heat exchangers in the preheater is given by:

$$LMTD_{ph} = T_{out} - T_f \tag{14}$$

Equations for the heat transfer coefficient in the evaporator and for the compressor work are given in El-Dessouky and Ettouney [11]. The overall heat transfer coefficient in the preheater (U_{ph}) was assumed to be 1.185 kW/m^2-K. This value was chosen to be consistent with the heat transfer coefficient within the MD module channels. The heat exchanger areas in the evaporator (A_{evap}) and the preheater (A_{ph}) are then obtained by dividing the respective heat transfer rates with the corresponding heat transfer coefficients.

Widely cited correlations from the literature were used to calculate equipment costs based on heat exchanger areas and compressor conditions [19,20]. These are:

$$\text{Cost}_{\text{evap}} = \$430 \times (0.582 U_{\text{evap}} A_{\text{evap}} \Delta P_{\text{t}}^{-0.01} \Delta P_{\text{s}}^{-0.1}) \quad (15)$$

$$\text{Cost}_{\text{ph}} = \$1000 \times (12.86 + A_{\text{ph}}^{0.8}) \quad (16)$$

$$\text{Cost}_{\text{comp}} = \$7364 \times \dot{m}_{\text{d}} \frac{P_{\text{cond}}}{P_{\text{evap}}} \left(\frac{\eta_{\text{comp}}}{1 - \eta_{\text{comp}}} \right)^{0.7} \quad (17)$$

where $\text{Cost}_{\text{evap}}$, Cost_{ph} and $\text{Cost}_{\text{comp}}$ are the costs of the evaporator/condenser, preheater, and compressor in units of US dollars, U_{evap} is the overall heat transfer coefficient in the evaporator in units of kW/m^2-K, A_{evap} and A_{ph} are the total areas of the evaporator and the preheat, respectively, in units of m^2, $\dot{m}_{\text{d}}$ is the mass flow rate of the vapor in the compressor in kg/s, ΔP_{t} and ΔP_{s} are the pressure drops on the tube and shell side of the evaporator/condenser in kPa. These correlations are not corrected for inflation or variations in raw material costs and are therefore used to obtain a rough estimate of the cost and understand the trends. The pressure drops are conservatively assumed to be 100 kPa. P_{cond} is the pressure in the condensing tubes while P_{evap} is the pressure in the evaporator, and η_{comp} is the isentropic efficiency of the compressor.

2.2. Performance metrics

In order to compare various MVC–MD hybrid systems, the overall cost savings by hybridization compared to using a stand-alone MVC system are evaluated.

The overall cost of water from the MVC–MD hybrid system is given by:

$$c_{\text{w}} = \frac{c'_{\text{w,MVC}} \dot{m}_{\text{p,MVC}} + c_{\text{w,MD}} \dot{m}_{\text{p,MD}}}{\dot{m}_{\text{p,total}}} \quad (18)$$

where $c'_{\text{w,MVC}}$ is the specific cost of water from the stand-alone MVC system per unit pure water production without including the cost of the brine-feed heat exchanger, in \$/m^3.

The overall heat transfer coefficient of the MD exchanger is lower than that of the heat exchanger due to the existence of the additional membrane resistance and gap thermal resistance. As a result, the area of MD required to achieve the same level of feed preheating is larger than the area of heat exchanger. The cost of water from MD $(c_{\text{w,MD}})$ is therefore defined as the sum of the amortized cost of the exchanger area (A_{MD}), cost of electricity for additional pumping, cost of maintenance (0.5% per annum of total CapEx), and the cost of membrane replacement at 10% per year. Amortization in both the MVC and MD cost models is based on a 20-year plant life at 8% rate of interest $(k_i = 1\%)$, and the calculations assume a 96% availability factor [5]. The baseline specific capital cost of the MD system (c_{MD}) is taken to be \$40/m^2.

The percentage of extra product produced by the hybrid system is given by $\dot{m}_{\text{p,MD}}/\dot{m}_{\text{p,MVC}} \times 100$. The percentage cost savings using the hybrid system is given by $c_{\text{w,MVC}} - c_{\text{w}}/c_{\text{w,MVC}} \times 100$. $c_{\text{w,MVC}}$ is higher than $c'_{\text{w,MVC}}$ since the cost of the brine-feed heat exchanger is also included.

The effect of several operating conditions on the cost of water from the hybrid system are then analyzed, including recovery ratio in the MVC stage, membrane permeability (B), MVC brine temperature, and c_{MD}.

3. Results and discussion

3.1. Overview of performance of proposed MVC–MD hybrid

The MVC–MD hybrid system proposed in this paper provides better performance than a conventional MVC system whenever the MD part of the system can cost-effectively produce extra product water. For a given MD system, more water can be produced if the vapor flux within the system is increased. Vapor flux in the MD is driven by the vapor pressure difference between the hot and cold streams; the larger the difference, the greater is the flux and the water produced. The vapor pressure difference itself depends on three factors: the mean temperature difference between the two streams (equivalent to LMTD_{ph}), the absolute temperature of the streams and the salinity of the streams. The vapor pressure difference between hot and cold streams in MD:

(a) Increases with an increase in LMTD_{ph}.
(b) Increases with the absolute temperature of the streams, since vapor pressure is an exponential function of temperature.
(c) Decreases with an increase in the salinity of the streams, since the vapor pressure of a saline fluid decreases with increasing salinity.

In the MVC–MD hybrid, variation in MD capital costs and the MD membrane permeability directly affect the MD system with little coupling with the MVC system performance. The former affects the cost-effectiveness of the water produced directly and the latter allows for a higher water production given the same temperature differences between hot and

cold streams. However, there is a strong coupling of the three factors described previously as well as between the MVC and MD systems, when the MVC parameters such as MVC recovery ratio (RR_{MVC}) and the MVC top brine temperature (T_{MVC}; but $T_{MVC} = T_b = T_{evap}$) are varied. When RR_{MVC} is increased (keeping other inputs constant), by definition, the product water or distillate produced per unit feed increases, while the amount of brine produced per unit feed decreases. The reduction in the brine mass flow rates thus reduces the amount of heat transfer possible in the MD component of the MVC–MD hybrid and largely reduces $\dot{m}_{p,MD}$ and the cost benefits of the MVC–MD hybrid. The reduction in the amount of heat transfer possible largely dominates over variations in other MD system parameters such as $LMTD_{ph}$. When T_{MVC} is increased, two competing effects occur: the $LMTD_{ph}$ decreases, whereas the absolute temperature of brine entering the preheater, T_b, increases. The former occurs because a higher T_{MVC} forces an increase in the effectiveness of heat transfer in the preheater, bringing T_{out} closer to the incoming feed temperature, T_f. For the ranges of T_{MVC} considered, the increase in T_b was found to dominate over the decrease in $LMTD_{ph}$ leading to a greater water production in the MD unit, $\dot{m}_{p,MD}$. A more detailed analysis of the effects introduced above is discussed in the sections below.

3.2. Effect of MVC recovery ratio

Fig. 4(a) shows the effect of the recovery ratio of the MVC system on the cost savings for CGMD, PGMD, and AGMD-based hybrid systems. Since we are considering the desalination of standard seawater, the recovery ratio in the MVC system would fully determine the salinity of the brine discharged to the MD unit. At a $RR_{MVC} = 0.5$, the cost savings with a CGMD hybrid system is about 6%. For much higher recovery ratios in the MVC section, the savings from the hybrid drop for all the configurations. This is a result of lower relative water production from the MD module compared to the MVC. At very high RR_{MVC}, the AGMD hybrid outperforms the CGMD hybrid, due to its higher η. At larger RR_{MVC}, the salinity of the brine leaving the evaporator is higher. As a result, η is significantly reduced for CGMD and PGMD, whereas, in the case of AGMD, the effect on η is lower.

Fig. 4(b) shows that the amount of extra product produced in the case of AGMD is higher than in the case of CGMD. This is a direct result of its higher η and lower conduction heat loss. Note that the total heat transfer in all three systems is equal, since the MD system area is allowed to vary to achieve the same extent of preheating that was achieved by the heat exchanger.

Fig. 5(a) shows the break-up of the total water cost which is a weighted sum of the cost of water from MVC and MD systems (Eq. (18)). The amount of water produced from MD is lower than 10% of the water produced in MVC, and hence the total cost is skewed closer to the specific cost of water for the MVC system. The cost of water from the MD part is a function of the specific membrane area. As RR_{MVC} increases, the salinity of water flowing into the MD system increases, but the expected temperature of the preheated feed reduces, leading to a larger driving force within the MD system. As a result, the specific MD area required decreases, before increasing due to salinity. Even

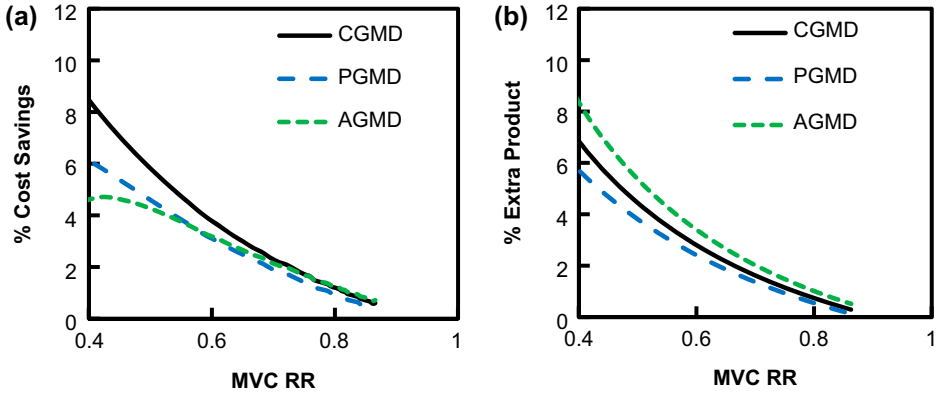

Fig. 4. (a) Effect of MVC recovery ratio on cost savings and (b) effect of MVC recovery ratio on the percentage of extra product produced by various systems.

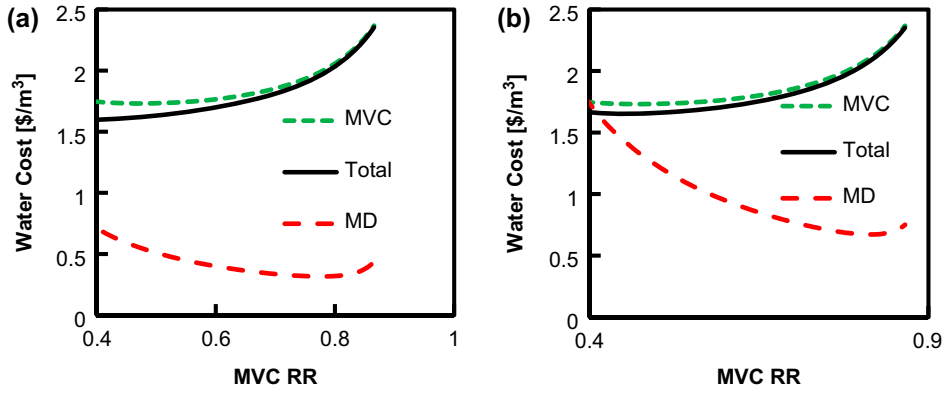

Fig. 5. (a) Effect of MVC recovery ratio on the water cost from stand-alone MVC, CGMD section, and hybrid system and (b) effect of MVC recovery ratio on the water cost from stand-alone MVC, AGMD section, and hybrid system.

though $c_{w,MD}$ is lower at higher RR_{MVC}, the relative savings are higher at lower RR_{MVC} due to the lower relative productivity of the MD section of the hybrid system at higher RR_{MVC} (as seen in Fig. 4(b)).

Fig. 5(b) shows a breakdown of the total cost of water for an AGMD hybrid system. The lower cost saving observed at low RR_{MVC} in the case of AGMD (Fig. 4(a)) is a result of the higher cost of water from MD that results from the higher specific membrane area requirement. This is a result of the lower $LMTD_{ph}$ requirement from the MD system at lower RR_{MVC}.

3.3. Effect of MVC top brine temperature

The effect of MVC top brine temperature is shown in Fig. 6(a). The savings from the hybrid system reach a maximum value before declining again at very high temperatures. Once again, the CGMD system outperforms other configurations due to its higher overall heat transfer coefficient and hence lower MD area requirement.

Fig. 6(b) shows the breakdown of the total cost of water for a MVC–CGMD hybrid system. At higher MVC operating temperature, the specific cost of water from MVC decreases. The recovery ratio is held constant ($RR_{MVC} = 0.5$) while the top temperature increases. At higher temperatures, the MVC model leads to a higher value of T_{ph}, with the value of $T_{MVC} - T_{ph}$ or $LMTD_{ph}$ decreasing. This results in a larger area requirement. At the same time, pure water production in the MD section increases at higher temperatures, leading to the total cost of water being pulled closer to the cost of MD (Eq. (18)). The overall effect of these two effects in the case of CGMD, over the temperature range considered in this study, is that the percentage savings increases with increase in T_{MVC}, reaching a maximum of around 7% at $T_{MVC} = 85$°C. In the case of AGMD and PGMD, a maximum is reached at a lower value of T_{MVC}.

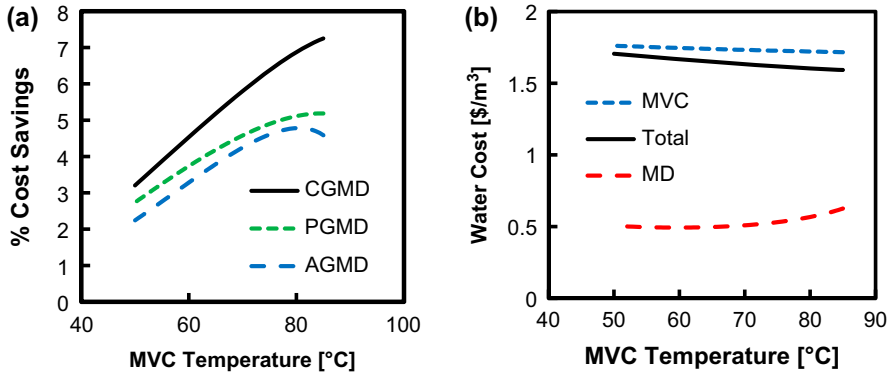

Fig. 6. (a) Effect of MVC operating temperature on cost savings and (b) effect of MVC operating temperature on water cost from stand-alone MVC, CGMD section and hybrid system.

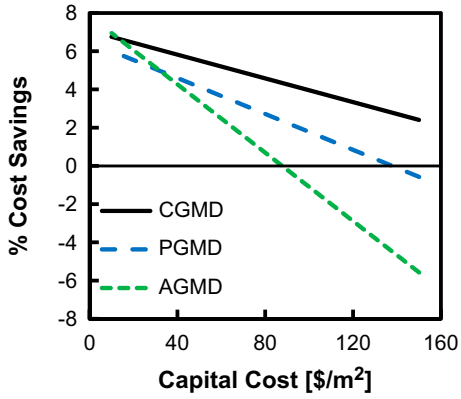

Fig. 7. Effect of MD specific cost on cost savings with various MD configurations.

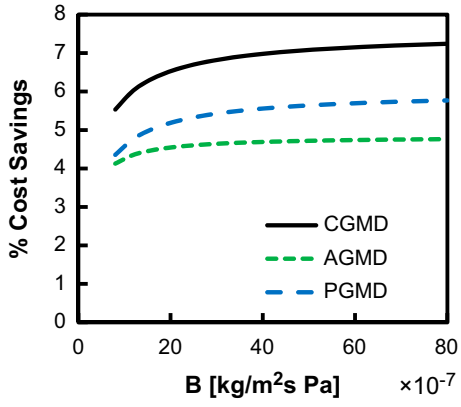

Fig. 8. Effect of MD membrane permeability on cost savings.

3.4. Effect of MD capital costs

The previous results are reported keeping the specific cost of MD area constant at \$40/m^2, irrespective of MD configuration type. Fig. 7 shows the effect of specific cost of MD system area on savings with a hybrid system. Since AGMD and PGMD require larger membrane area, at larger specific system cost, these systems result in no cost savings. At a very low cost of the MD system, the fact that AGMD needs larger area is offset by the higher water productivity of AGMD compared to CGMD, leading to more savings in the case of AGMD compared to CGMD.

3.5. Effect of MD membrane permeability

The membrane transfer coefficient is a function of the specific MD membrane used, as well as operating conditions such as temperature. B increases with: an increase in temperature, a decrease in membrane thickness, and an increase in porosity or pore size. Fig. 8 shows that the savings for CGMD and PGMD hybrid systems are more significantly affected by B than AGMD. This is because in the case of AGMD, the air gap constitutes the major thermal resistance, whereas in CGMD, the membrane is the major thermal resistance.

Fig. 9(a) shows the effect of membrane permeability on water productivity and MD area requirement. At higher B, the thermal efficiency (η) increases in the case of CGMD and PGMD, leading to greater water production in the MD section, for the same extent of preheating or overall heat transfer. Fig. 9(b) shows the effect of B on MD area requirements. The effect of the overall heat transfer coefficient can be observed, with the area requirement of AGMD being about three times and that

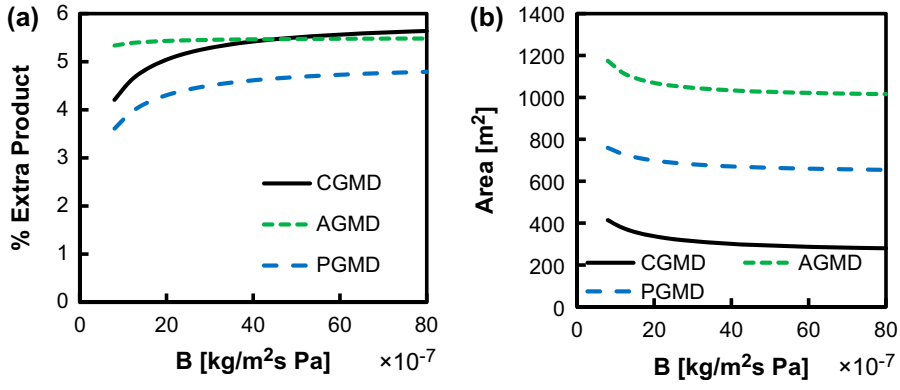

Fig. 9. (a) Effect of MD membrane permeability on percentage of extra product and (b) effect of MD membrane permeability on membrane area requirement.

of PGMD about two times higher than that of CGMD. For all the systems, with an increase in membrane permeability, the total area requirement decreases. These effects together influence the cost of water from MD by affecting the specific membrane area requirement. The specific cost of water from MD, along with the amount of water produced in the MD system, determines the overall cost savings illustrated in Fig. 8.

4. Conclusions

(1) MD modules can be used in the place of heat exchangers in a MVC system, to produce additional pure water while achieving preheating of the feed stream using the hot brine.
(2) Keeping the MVC system operating conditions constant, the cost of water production can be reduced up to 8% by hybridizing MVC and CGMD.
(3) Conductive gap MD has maximum overall heat transfer coefficient, U, leading to lower area requirements, and higher savings than for other systems over a wide range of operating conditions. At very high salinities, or low cost of MD system, air gap MD outperforms CGMD in due to its lower heat loss.
(4) If the specific cost of the MD system is lower than about US\$40/m^2, a cost savings of about 4–8% can be achieved with either AGMD or CGMD hybridization for a 50% recovery seawater MVC system operating at 70°C.

Acknowledgments

This work was funded by the Cooperative Agreement Between the Masdar Institute of Science and Technology (Masdar Institute), Abu Dhabi, UAE and the Massachusetts Institute of Technology (MIT), Cambridge, MA, USA, Reference No. 02/MI/MI/CP/11/07633/GEN/G/00, and facilitated by the MIT Deshpande Center for Technological Innovation and the Masdar Institute Center for Innovation and En-trepreneurship (iInnovation).

References

[1] J. Swaminathan, H.W. Chung, D.M. Warsinger, J.H. Lienhard V, Simple method for balancing direct contact membrane distillation, Desalination 383 (2016) 53–59, 0011-9164, doi: 10.1016/j.desal.2016.01.014.
[2] M.I. Hassan, A.T. Brimmo, J. Swaminathan, J.H. Lienhard V, H.A. Arafat, A new vacuum membrane distillation system using an aspirator: Concept modeling and optimization, Desalin. Water Treat. 57 (28) (2016) 12915–12928, doi: 10.1080/19443994.2015.1060902.
[3] H.W. Chung, J. Swaminathan, D.M. Warsinger, J.H. Lienhard V, Multistage vacuum membrane distillation (MSVMD) systems for high salinity applications, J. Membr. Sci. 497 (2016) 128–141, doi: 10.1016/j.memsci.2015.09.009.
[4] E.K. Summers, H.A. Arafat, J.H. Lienhard V, Energy efficiency comparison of single-stage membrane distillation (MD) desalination cycles in different configurations, Desalination 290 (2012) 54–66, doi: 10.1016/j.desal.2012.01.004.
[5] R.B. Saffarini, E.K. Summers, H.A. Arafat, J.H. Lienhard V, Economic evaluation of stand-alone solar powered membrane distillation systems, Desalination 299 (2012) 55–62, doi: 10.1016/j.desal.2012.05.017.
[6] K.H. Mistry, R.K. McGovern, G.P. Thiel, E.K. Summers, S.M. Zubair, J.H. Lienhard V, Entropy generation analysis of desalination technologies, Entropy 13 (2011) 1829–1864, doi: 10.3390/e13101829.
[7] D.M. Warsinger, J. Swaminathan, E. Guillen-Burrieza, H.A. Arafat, J.H. Lienhard V, Scaling and fouling in membrane distillation for desalination applications: A review, Desalination 356 (2015) 294–313, doi: 10.1016/j.desal.2014.06.031.
[8] E.K. Summers, J.H. Lienhard V, A novel solar-driven air gap membrane distillation system, Desalin. Water Treat. 51 (2012) 1–8, doi: 10.1080/19443994.2012.705096.
[9] J. Swaminathan, H.W. Chung, D.M. Warsinger, F. Al-Marzooqi, H.A. Arafat, J.H. Lienhard V, Energy efficiency of permeate gap and novel conductive gap membrane distillation, J. Membr. Sci. 502 (2016) 171–178, doi: 10.1016/j.memsci.2015.12.017.
[10] J. Swaminathan, H.W. Chung, D.M. Warsinger, J.H. Lienhard V, Heat exchanger theory based membrane distillation model and module comparison (under review), 2016.
[11] H.T. El-Dessouky, H.M. Ettouney, Fundamentals of Salt Water Desalination, Elsevier, Amsterdam, 2002.
[12] H. Ettouney, Design of single-effect mechanical vapor compression, Desalination 190 (2006) 1–15, doi: 10.1016/j.desal.2005.08.003.
[13] D.M. Warsinger, K.H. Mistry, K.G. Nayar, H.W. Chung, J.H. Lienhard V, Entropy generation of desalination powered by variable temperature waste heat, Entropy 17 (2015) 7530–7566, doi: 10.3390/e17117530.
[14] N.H. Aly, A.K. El-Figi, Mechanical vapor compression desalination systems—A case study, Desalination 158 (2003) 143–150, doi: 10.1016/S0011-9164(03)00444-2.
[15] S.A. Klein, F.L. Alvarado, Engineering Equation Solver, F-Chart Software, Madison, WI, 1, 2002.
[16] A.L. Zydney, Stagnant film model for concentration polarization in membrane systems, J. Membr. Sci. 130 (1997) 275–281, doi: 10.1016/S0376-7388(97)00006-9.
[17] G.P. Thiel, E.W. Tow, L.D. Banchik, H.W. Chung, J.H. Lienhard, Energy consumption in desalinating produced water from shale oil and gas extraction, Desalination 366 (2014) 94–112, doi: 10.1016/j.desal.2014.12.038.

[18] J. Veza, Mechanical vapour compression desalination plants—A case study, Desalination 101 (1995) 1–10, doi: 10.1016/0011-9164(95)00002-J.
[19] Y.M. El-Sayed, Designing desalination systems for higher productivity, Desalination 134 (2001) 129–158, doi: 10.1016/S0011-9164(01)00122-9.
[20] A.S. Nafey, H.E.S. Fath, A.A. Mabrouk, Thermoeconomic design of a multi-effect evaporation mechanical vapor compression (MEE–MVC) desalination process, Desalination 230 (2008) 1–15, doi: 10.1016/j.desal.2007.08.021.